PHILOSOPHICAL TRANSACTIONS A

royalsocietypublishing.org/rsta

CC BY

Research

Cite this article: Zheng Y, Xie H, Wang X, Yang F, Boers N. 2026 Impact of non-symmetric α-stable Lévy processes on mean exit time in abrupt climate transitions. *Phil. Trans. R. Soc. A* **384**: 20240488.
https://doi.org/10.1098/rsta.2024.0488

Received: 22 February 2025
Accepted: 29 August 2025

One contribution of 13 to a theme issue 'Critical transitions and intelligent control in complex systems'.

Subject Areas:
climatology, mathematical modelling

Keywords:
non-symmetric α-stable lévy processes, mean exit time, abrupt climate transitions, greenhouse effect

Author for correspondence:
Yayun Zheng
e-mail: zhengyayun@ujs.edu.cn

Impact of non-symmetric α-stable Lévy processes on mean exit time in abrupt climate transitions

Yayun Zheng[1], Hao Xie[1], Xiao Wang[2], Fang Yang[3] and Niklas Boers[4,5,6]

[1]Jiangsu University, Zhenjiang 212013, People's Republic of China
[2]Henan University, Kaifeng 475001, People's Republic of China
[3]Basic Department, Information Engineering University, Zhengzhou 450001, People's Republic of China
[4]Technical University of Munich, Munich 85521, Germany
[5]Potsdam Institute for Climate Impact Research (PIK), Potsdam 14473, Germany
[6]University of Exeter, Exeter EX4 4SB, UK

YZ, 0000-0002-7725-379X

Abrupt climate change involves rapid transitions between alternative stable states in the Earth's climate system, posing significant risks to global stability. Recent concerns suggest that such transitions could be triggered by individual extreme events, yet the underlying mechanisms remain poorly understood. In this study, we investigate these mechanisms using a stochastic energy balance model that incorporates extreme weather events through a non-symmetric α-stable Lévy process. Our analysis highlights the critical role of the non-symmetric Lévy parameters in shaping system dynamics. Specifically, the stability parameter α governs the frequency and intensity of extreme events: smaller α values lead to larger but less frequent extreme events, significantly shortening the mean exit time (MET) of the system. Furthermore, the skewness parameter β determines the asymmetric distribution of extreme events, with its impact highly dependent on tail heaviness: environments dominated by heavy-tailed ($\alpha < 1$) and skewed ($\beta \neq 0$) extreme events can reduce system stability. In addition, we observe that the enhanced greenhouse effect increases the sensitivity of the cold state, further

© 2026 The Authors. Published by the Royal Society under the terms of the Creative Commons Attribution License http://creativecommons.org/licenses/by/4.0/, which permits unrestricted use, provided the original author and source are credited.

THE ROYAL SOCIETY PUBLISHING

Downloaded from royalsocietypublishing.org/rsta/article-pdf/doi/10.1098/rsta.2024.0488/6160760/rsta.2024.0488.pdf
by guest
on 11 November 2026

destabilizing it. Our work highlights the importance of considering heavy-tailed, non-symmetric stochastic processes in understanding and predicting climate system stability.

This article is part of the theme issue 'Critical transitions and intelligent control in complex systems'.

1. Introduction

Certain components of the Earth system are capable of undergoing abrupt state changes in response to gradual external forcing [1,2]. This phenomenon has attracted substantial scientific attention in recent years and is widely regarded as one of the most pressing threats associated with climate change [3–5]. Empirical evidence for such abrupt transitions primarily comes from paleoclimate proxy records. Greenland ice core data reveal that during the last glacial period, the climate experienced nearly 30 rapid transitions between a cold glacial state and a warmer interstadial one, commonly referred to as Dansgaard–Oeschger events [6,7]. These events are characterized by rapid temperature increases over Greenland of up to 16°C occurring within just a few decades, followed by gradual cooling [8,9].

Despite extensive research, the underlying mechanisms driving these abrupt climate transitions remain unclear. Among the proposed explanations, bifurcation-induced transition has been identified as one of several tipping mechanisms responsible for such shifts [10,11]. In addition, noise-induced transitions can also trigger irregular and unpredictable state changes when random fluctuations are sufficiently large [12,13]. These random fluctuations, often referred to as noise, represent external atmospheric forcing, such as wind stress, heat exchange or freshwater transport, all of which play a significant role in influencing the climate state [14]. Traditionally, such noise has been modelled as a Gaussian process in climate simulations [15]. Gaussian processes lead to continuous evolutions with a light tail, following an exponential distribution, and are widely used for model performance and testing from data [16–18].

However, Ditlevsen's analysis of paleoclimate data suggests that these rapid, heavy-tailed fluctuations often exhibit non-Gaussian characteristics [19]. Consequently, an α-stable Lévy process provides a more appropriate framework for modelling these extreme events [20]. Unlike Gaussian noise, Lévy processes are inherently discontinuous and unpredictable, following a power-law distribution [21]. These properties make the Lévy process particularly suitable for capturing the statistical features of abrupt climate transitions driven by extreme fluctuations.

To investigate the effect of noise on the transition behaviour of climate systems, we focus on the mean exit time (MET) as a global measure to quantify the stability of the climate system. The MET represents the expected time for the system to cross a critical threshold, such as the boundary of a given basin of attraction [22,23]. This measure is widely applicable and has been employed to analyse the stability of various systems, including financial markets [24], genetic transcriptional networks [25] and geoscience systems [26,27]. In the small-noise limit, large deviation theory provides a theoretical framework for approximating the MET. Specifically, the classic Arrhenius formula gives an analytical expression for the MET's decay exponent [22]. For finite noise intensity, the evolution of the MET can be described by solving an elliptic partial differential equation subject to specific boundary conditions [28,29], such as absorbing boundaries (Dirichlet boundaries) [22] or a combination of absorbing and reflecting boundaries (Dirichlet–Neumann boundaries) [27].

Recent advancements have extended these theoretical approaches to systems driven by non-Gaussian noise, such as the α-stable Lévy process. It is shown that the MET increases with a power $\epsilon^{-\alpha}$ of the noise intensity ϵ [30,31]. Efficient and accurate numerical schemes have been developed and validated for computing the MET under such processes [32]. Furthermore, the skewness parameter β has been found to significantly influence the probability distribution of stable Lévy random variables, highlighting the asymmetric nature of these processes. Building on these insights, Wang *et al.* [33] proposed a refined numerical method for computing the MET in stochastic

Downloaded from royalsocietypublishing.org/rsta/article-pdf/doi/10.1098/rsta.2024.0488/6160760/rsta.2024.0488.pdf
by guest
on 11 November 2026

systems driven by asymmetric Lévy process, further advancing our understanding of noise-induced transitions in complex systems.

The primary objective of this study is to evaluate how extreme events, coupled with the greenhouse effect [35], may interact to trigger abrupt transitions from a cold to a warm state. The paper is structured as follows. In §2, we provide an overview of the Lévy process $L(t)$ and discuss the MET for stochastic systems driven by an asymmetric Lévy process. A conceptual stochastic energy balance model is introduced to describe climate dynamics under the influence of extreme events. In §3, we present numerical experiments on the effects of the stability parameter α, the skewness parameter β and the greenhouse effect factor on the MET. Finally, we summarize our findings and discuss their implications for understanding abrupt climate transitions.

2. Method and model

(a) α-stable Lévy process

A Lévy process $L(t)$ is a non-Gaussian process with stationary and independent increments. The sample paths are almost surely right-continuous with left limits, i.e. have countable jumps. Lévy processes are thought to be an appropriate model for non-Gaussian fluctuations with heavy-tailed distribution and intermittent bursts. A scalar Lévy motion L_t with triplet (b, Q, ν) is completely determined by the Lévy–Khintchine formula [21]:

$$Ee^{iuL_t} = \exp\left\{ ibut - Qt\frac{u^2}{2} + t\int_{\mathcal{R}^1\setminus\{0\}} (e^{iuy} - 1 - iuyI_{|y|<1})\nu(dy)\right\} \quad u \in \mathcal{R}^1,$$

which is characterized by a linear coefficient b, a non-negative variance parameter Q and a non-negative Borel measure ν defined on $\mathcal{R}^1 \setminus \{0\}$, which satisfies $\int_{\mathcal{R}^1\setminus\{0\}}(|y|^2 \bigwedge 1)\nu(dy) < \infty$.

An α-stable Lévy process is a special type of Lévy process defined by the stable Lévy random variable with distribution $S_\alpha(\sigma, \beta, \mu)$ [34]. The four real parameters are the stability parameter $\alpha \in (0, 2)$, the skewness parameter $\beta \in [-1, 1]$, the scalar parameter $\sigma > 0$ and the shift parameter μ. Figure 1*a* illustrates the tail characteristics of stable Lévy random variables. When the stability parameter α lies in the range $0 < \alpha < 2$, such as $\alpha = 1$ (grey line), which corresponds to the Cauchy distribution, these variables exhibit 'heavy-tail' behaviour. The probability follows a power-law decay [21,34], expressed as

$$\mathbb{P}(|L^\alpha(t)| > y) \sim \frac{1}{y^\alpha}.$$

By contrast, for $\alpha = 2$ (yellow line), the stable random variable corresponds to the well-known normal Gaussian distribution, which features a 'light tail', as tail probability decays exponentially [22].

The skewness parameter β has a significant influence on the probability distribution of a stable Lévy random variable. Figure 1*b*,*c* illustrates how the parameter β determines the skewness of the stable Lévy random variable's distribution: it skews to the left-hand side when $\beta < 0$ (indicating that the tail is on the left-hand side of the distribution), and to the right-hand side when $\beta > 0$ (indicating that the tail is on the right-hand side).

Next, we focus on studying a stochastic dynamical system driven by an asymmetric α-stable Lévy process:

$$dX_t = f(X_t)dt + dL_t^{\alpha,\beta}, \quad X_0 = x_0 \in \mathcal{R}^1. \tag{2.1}$$

Here, $L_t^{\alpha,\beta}$ is a scalar α-stable Lévy process with generating triplet $(0, 0, \epsilon\nu_{\alpha,\beta})$, and ϵ is a Lévy noise intensity. If the function f is a vector field, satisfying both the Lipschitz condition and the linear

Downloaded from royalsocietypublishing.org/rsta/article-pdf/doi/10.1098/rsta.2024.0488/6160760/rsta.2024.0488.pdf
by guest
on 11 November 2026

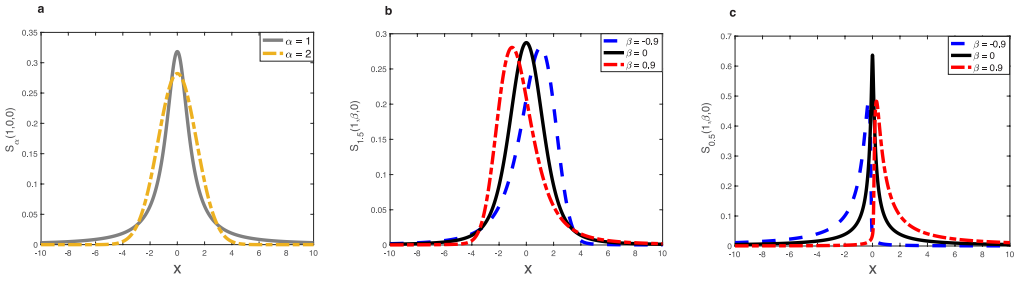


Figure 1. The stable Lévy random variable distribution $S_\alpha(\sigma, \beta, \mu)$. (a)The tail behaviour of the symmetric stable Lévy random variable for $\alpha = 1$ and $\alpha = 2$. (b) The skewness distribution of the stable Lévy random variable with $\alpha = 1.5$ and $\beta = -0.9, 0, 0.9$. (c) Same as (b) except $\alpha = 0.5$.

growth condition, then the solution $X(t)$ of stochastic differential equation (SDE) (equation (2.1)) exists and is unique [21].

The generator $\mathcal{L}$ of the solution process X_t in equation (2.1) is defined by [23]:

$$\mathcal{L}\phi = f(x)\phi'(x) + \epsilon \int_{R\setminus\{0\}} [\phi(x+y) - \phi(x) - I_{|y|<1}(y)y\phi'(x)]\nu_{\alpha,\beta}(dy), \tag{2.2}$$

where asymmetric α-stable Lévy jump measure $\nu_{\alpha,\beta}$ is defined by

$$\nu_{\alpha,\beta}(dy) = \frac{C_1 1_{\{0<y<\infty\}}(y) + C_2 1_{\{-\infty<y<0\}}}{|y|^{1+\alpha}}(dy),$$

with $\beta = (C_1 - C_2)/(C_1 + C_2)$, $C_1 = C_\alpha \frac{1+\beta}{2}$ and $C_2 = C_\alpha \frac{1-\beta}{2}$, where

$$C_\alpha = \begin{cases} \frac{\alpha(1-\alpha)}{\gamma(2-\alpha)cos(\frac{\pi\alpha}{2})}, & \alpha \neq 1, \\ \frac{\pi}{2}, & \alpha = 1. \end{cases}$$

(b) Mean exit time

The MET is a deterministic measure used to describe the stochastic behaviour of a dynamical system. For a bounded domain $D = (a, b) \in R^1$, the first exit time for the solution of equation (2.1), starting at a point $x \in D$, is defined as

$$\tau(x, \omega) \triangleq inf\{t \geq 0, X_t(x, \omega) \notin D\}.$$

It is known that $\tau(x, \omega)$ is a stopping time. The MET is defined as the mean residence time of the system, initially located at x, until it first exits the domain D:

$$u(x) \triangleq E\tau(x, \omega) \geq 0.$$

By Dynkin's formula for Markov processes, the MET satisfies the following elliptic differential equation with absorbing boundary conditions [23,29]:

$$\begin{cases} \mathcal{L}u = -1, & x \in D, \\ u(x) = 0, & x \in D^c, \end{cases} \tag{2.3}$$

where the generator $\mathcal{L}$ is defined in equation (2.2).

Wang *et al.* [33] proposed a numerical finite-difference scheme for solving the MET in stochastic systems driven by an asymmetric Lévy process. This scheme is derived from the

Downloaded from royalsocietypublishing.org/rsta/article-pdf/doi/10.1098/rsta.2024.0488/6160760/rsta.2024.0488.pdf
by guest
on 11 November 2026

differential-integral equation (2.3) on the interval $s \in (-1, 1)$. In this paper, we employ Wang's numerical method for the MET in asymmetric Lévy processes. Specifically, for the numerical calculations presented in this work, the solution for the MET over an arbitrary domain $D = (a, b)$ is obtained by applying a scalar transformation defined as $x = \frac{b-a}{2}s + \frac{a+b}{2}$.

(c) Stochastic energy balance model

A concept energy balance model has been proposed to describe climate change through the evolution of the global mean surface temperature $T(t)$ [36,37]. This model captures the temperature dynamics as governed by the difference between incoming solar radiation and outgoing radiation at any given time t,

$$C\frac{dT}{dt} = \frac{S_0}{4}(1 - \alpha(T)) - \gamma\theta T^4, \tag{2.4}$$

where $C = 46.8$ W yr m^{-2} denotes the heat capacity of the system, representing a weighted average of the ability of the ocean and land surface to store heat in response to a one kelvin temperature increase [38]. The first term on the right-hand side of the equation represents the total amount of solar radiation absorbed by the Earth after reflection with the solar constant $S_0 = 1368$ W m^{-2}. The albedo is temperature-dependent and is defined as

$$\alpha(T) = 0.5 - 0.2\tanh\left(\frac{T - 265}{10}\right).$$

The second term accounts for the radiative energy loss from the Earth's surface, modelled using the Stephen–Boltzmann law θT^4, where the Stephen–Boltzmann constant is given by $\theta = 5.67 \times 10^{-8}$W yr m^{-2}. In addition, the absorbed energy by greenhouse gases leads to an increase in global average temperature. To maintain energy balance, we use the greenhouse effect factor $\gamma \in (0, 1)$ to represent the reduction in outgoing energy.

By setting the right-hand side of the energy balance model (equation (2.4)) to 0, all equilibrium states can be determined. Figure 2*a* illustrates the graphs of equilibrium states in the climate change model based on the bifurcation parameter γ. For greenhouse effect factors below $\gamma_f = 0.49$, the Earth system remains in a high-temperature state, while, for above $\gamma_h = 0.69$, the temperature is almost exclusively a cold state, referred to as a 'Snowball Earth', characterized by long-time stabilization in an ice-covered state [39]. For $0.49 < \gamma < 0.69$, the climate system exhibits bistable behaviour. Specifically, when $\gamma = 0.55$, the system has a warm stable state $T_w = 296$ K, a cold one $T_c = 240$ K and an unstable state $T_u = 261$ K. This implies that the global surface temperature T increases as the greenhouse factor γ decreases. Thus, a reduction in the greenhouse effect factor enhances the greenhouse effect, leading to a rise in the global mean surface temperature.

The potential function governing these dynamics can be expressed as $dT = -U(T)dt$, where the potential function $U(T)$ is defined as

$$U(T) = -\frac{S_0}{4}\left(0.5T + 2\ln\left(\cosh\left(\frac{T - 265}{10}\right)\right)\right) + \frac{1}{5}\gamma\theta T^5.$$

We select two representative values of γ within the bistable region: $\gamma = 0.55$ and $\gamma = 0.67$. Figure 2*c* shows the potential function at $\gamma = 0.67$, revealing a deeper potential well for the cold state, which indicates that the cold state is more stable. Conversely, the potential function at $\gamma = 0.55$ demonstrates the opposite result, as shown in figure 2*b*.

Extreme weather events, such as heat waves, storms and freshwater, have been shown to serve as triggering mechanisms for abrupt climate change [40,41]. The occurrence of these extreme weather events aligns with discrete disturbance events that occur as abrupt burst-like pulses, which can be characterized by a heavy-tailed distribution. This can be effectively approximated by a Lévy process. Therefore, the climate system influenced by extreme weather events can be

Downloaded from royalsocietypublishing.org/rsta/article-pdf/doi/10.1098/rsta.2024.0488/6160760/rsta.2024.0488.pdf
by guest
on 11 November 2026

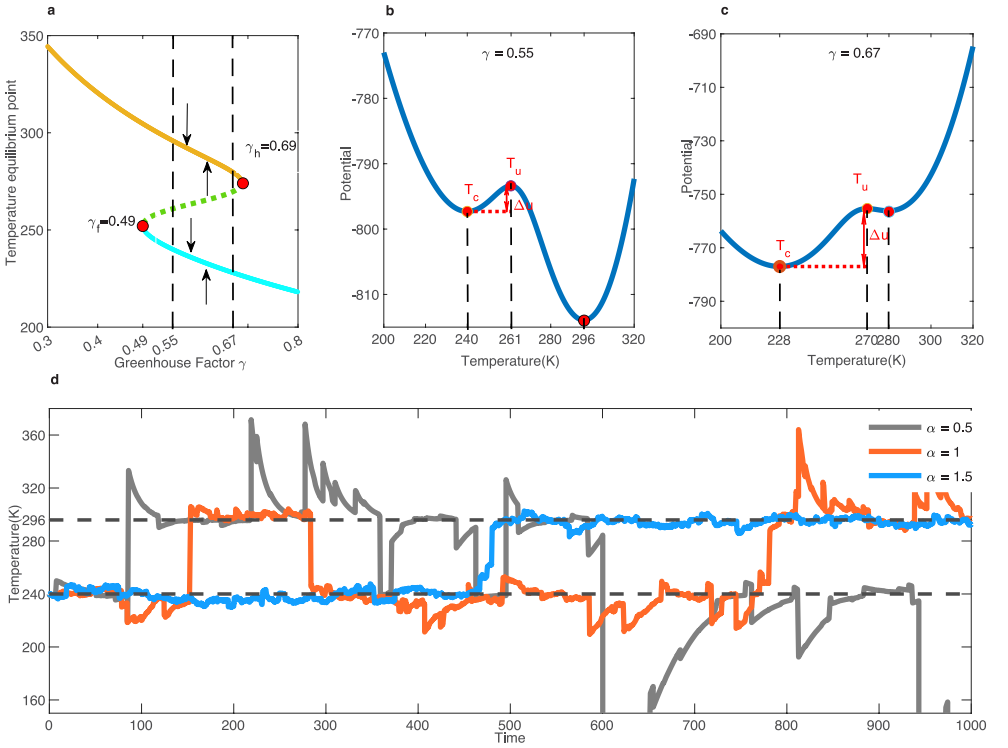


Figure 2. (a) Bifurcation diagram of equilibrium states in the climate change model equation (2.4). The cold states are represented by the blue line, and the warm ones are represented by the yellow line. The climatic system exhibits the two stable states for $0.49 < \gamma < 0.69$ (Bistable region). The potential functions $U(T)$ at the greenhouse effect factors: (b) $\gamma = 0.55$ and (c) $\gamma = 0.67$. (d) The stochastic sample paths of climate change for $\gamma = 0.55$ in equation (2.5) using the Euler–Maruyama scheme for $\alpha = 0.5$, $\alpha = 1$ and $\alpha = 1.5$.

modelled by the following SDE driven by an asymmetric α-stable Lévy process:

$$dT = \frac{1}{C}\left(\frac{S_0}{4}(1-\alpha(T)) - \gamma\theta T^4\right)dt + dL_t^{\alpha,\beta}. \tag{2.5}$$

The SDE has a unique solution owing to the drift term satisfying the Lipschitz and linear growth conditions; $L_t^{\alpha,\beta}$ represents a scalar asymmetric α-stable Lévy process with the triplet $(0, 0, \epsilon\nu_{\alpha,\beta})$. Here, the stability parameter $\alpha \in (0, 2)$ and the skewness parameter $\beta \in (-1, 1)$. In the following study, we set the noise intensity $\epsilon = 0.5$.

Figure 2*d* shows the stochastic sample paths of climate change for $\gamma = 0.55$, which are simulated using the Euler–Maruyama scheme with a time step of $\Delta t = 0.01$. The sample paths illustrate non-Gaussian noise-induced transitions from the cold state $T_c = 240$ K through the unstable state $T_u = 261$ K to the warm state $T_w = 296$ K. For smaller values of α, such as $\alpha = 0.5$ (grey line), the trajectory displays large jumps at low frequencies. While for α values close to two, such as $\alpha = 1.5$ (blue line), the trajectory makes smaller jumps with higher probabilities. This implies that the α-stable Lévy process can effectively quantify the frequency and intensity of extreme events.

3. Result

Now, we analyse the impact of the frequency and intensity of extreme weather events on the stability of the climate system by examining the influence of the stability parameter α and skewness parameter β on the MET in equation (2.3).

Downloaded from royalsocietypublishing.org/rsta/article-pdf/doi/10.1098/rsta.2024.0488/6160760/rsta.2024.0488.pdf
by guest
on 11 November 2026

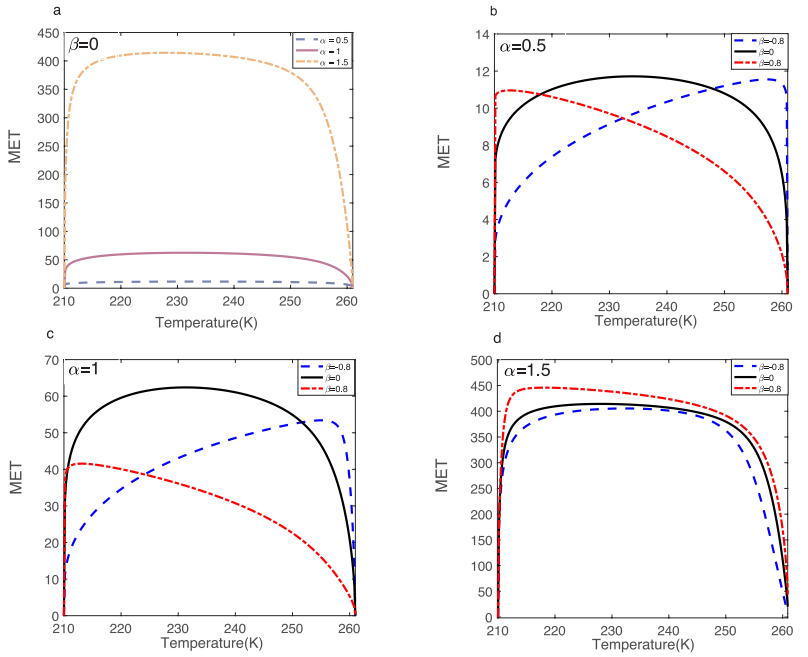


Figure 3. The effect of α and β on MET within the cold basin of attraction $D = (210, 261)$ for $\epsilon = 0.5$ and $\gamma = 0.55$. (a) $\alpha = 0.5, 1, 1.5$ with $\beta = 0$. (b) $\beta = -0.8, 0, 0.8$ with $\alpha = 0.5$. (c) Same as (b) except $\alpha = 1$. (d) Same as (b) except $\alpha = 1.5$.

(a) The effect of α and β on mean exit time within the cold attraction basin

Figure 3 illustrates the impact of the stability parameter α and the skewness parameter β on the MET within the cold state attraction basin $D = (210, 261)$ for the greenhouse effect factor $\gamma = 0.55$. For $\beta = 0$, fixed, figure 3*a* shows that α increases, the MET grows significantly, indicating that the system requires more time to exit from the cold state to the warm one in the climate system. This behaviour indicates that the system becomes more stable as larger α corresponds to smaller jumps with higher probabilities for extreme events.

The skewness parameter β governs the asymmetry of the α-stable Lévy random variable's distribution. A left-skewed distribution, characterized by its tail extending to the left, is observed when $\beta < 0$. Conversely, when $\beta > 0$, the distribution is right-skewed, with its tail extending to the right. We compare three representative values of β, that is, -0.8, 0 and 0.8. The numerical results reveal differential temperature dependencies on MET in the varying stability parameter α. Specifically, for $\alpha = 1.5$, as shown in figure 3*d*, a value characteristic of a Lévy process dominated by frequent, small jumps, the MET demonstrates a monotonic increase with β increasing. By contrast, for $\alpha = 0.5$ and $\alpha = 1$, as shown in figure 3*b*,*c*, the relationship between β and the MET exhibits a more complex regime-dependent behaviour.

(b) The effect of α and β on the mean exit time at the cold metastable state

To examine the interaction between MET and fluctuations, the study investigates the combined effects of the stability parameter α and the skewness parameter β on MET. This analysis focuses on the system's transition to the warm state, starting from the cold metastable state $T_c = 240$ K for $\gamma = 0.55$.

Figure 4 represents the dependence of MET on β and α, revealing a non-monotonic trend. For a fixed range of $\beta \in (-1, 1)$, it is further detailed by segmenting the parameter α into three distinct regimes. For $\alpha \in (0, 1)$, as shown in figure 4*a*, MET consistently exhibits a 'bell-shaped' curve with

Downloaded from royalsocietypublishing.org/rsta/article-pdf/doi/10.1098/rsta.2024.0488/6160760/rsta.2024.0488.pdf
by guest
on 11 November 2026

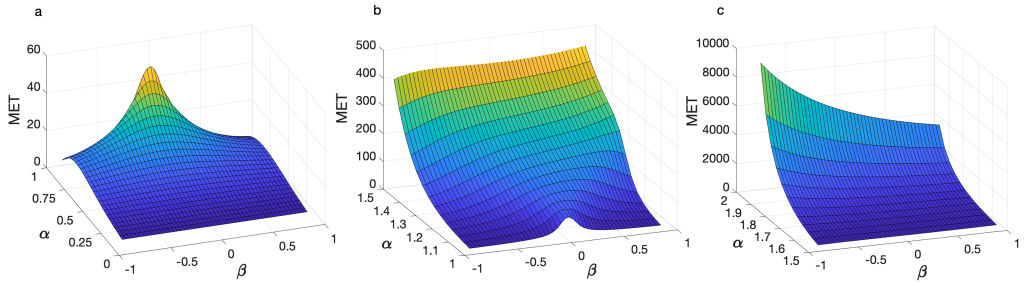


Figure 4. The influence of α and β on MET at the stable cold state $T_c = 240$ K for $\gamma = 0.55$, fixed $\epsilon = 0.5$ and $\beta \in (-1, 1)$. The stability parameter α is divided into three distinct regimes. (a) $\alpha \in (0, 1)$. (b) $\alpha \in (1, 1.5)$. (c) $\alpha \in (1.5, 2)$.

a peak located around $\beta = 0$. As α increases with the range $(1, 1.5)$ (figure 4*b*), the dependency of MET on β transfers from a unimodal profile to a wavy pattern. Furthermore, as α approaches 2, the system displays Gaussian-like behaviour, and MET with respect to β shows a monotonically decreasing trend.

These findings suggest that the impact of noise characteristics on system MET varies across different regimes of tail heaviness. Specifically, in environments dominated by extreme heavy-tailed events, maximum system MET is achieved when the noise is symmetric. Conversely, for systems exhibiting moderately heavy-tailed characteristics, a skewness in the underlying driving forces may potentially enhance stability. Furthermore, for systems approaching Gaussian dynamics (less extreme natural variability), the introduction of any positive skewness consistently shortens the mean time for the system to exit its desired climatic state. This, in turn, significantly reduces the system's stability and increases the likelihood of rapid transitions to unfavourable climate states.

(c) Dependence of α and β on mean exit time for strong and weak greenhouse effect

Next, we investigate the transition behaviour of the climate system under two different strengths of the greenhouse effect: a relatively weak greenhouse effect $\gamma = 0.67$ and a strong one $\gamma = 0.55$. We focus on the MET starting from the cold metastable state $T_c = 228$ K for $\gamma = 0.67$ compared with the cold one $T_c = 240$ K for $\gamma = 0.55$. Figure 5*a–d* illustrates the dependence of the MET on the skewness parameter $\beta \in [-0.9, 0.9]$ for two different strengths of the greenhouse effect and the four typical values of $\alpha = 0.5, 1, 1.5, 1.9$.

A comparative analysis of MET trends with respect to β for $\gamma = 0.67$ and $\gamma = 0.55$ reveals broadly similar behaviours. Specifically, for $\alpha = 0.5$ and $\alpha = 1$, both exhibit a stable bell-shaped curve, which transitions to a monotonic trend as α approaches two. However, a crucial distinction emerges from the four subfigures: when $\beta > 0$, which corresponds to a left-skewed α-stable Lévy random distribution (figure 1*b*), the MET for $\gamma = 0.55$ is consistently lower than that for $\gamma = 0.67$. By contrast, for $\beta < 0$, the opposite relationship is true. These findings indicate that the cold state associated with a stronger greenhouse effect ($\gamma = 0.55$) inherently possesses reduced stability compared to that with a weaker greenhouse effect ($\gamma = 0.67$). Furthermore, under the influence of the right-skewed noise, the stability of the cold state for the stronger greenhouse effect ($\gamma = 0.55$) is further diminished, potentially leading to significant impacts on the global climate dynamics.

To further explore the impact of noise characteristics, we vary the value of α from 0.1 to 1.9 while setting $\beta = -0.5, 0, 0.5, 0.9$, respectively. Figure 5*d–g* shows that the MET increases rapidly as α approaches 2 for all values of β, in agreement with the corresponding result in the MET increases with a power $\epsilon^{-\alpha}$ [30,31]. This reflects the stabilizing effect of smaller noise jumps. From the perspective of the skewness parameter β, for symmetric noise ($\beta = 0$), the climate system exhibits similar behaviour under the influence of the two greenhouseeffects. However, for asymmetric

Downloaded from royalsocietypublishing.org/rsta/article-pdf/doi/10.1098/rsta.2024.0488/6160760/rsta.2024.0488.pdf
by guest
on 11 November 2026

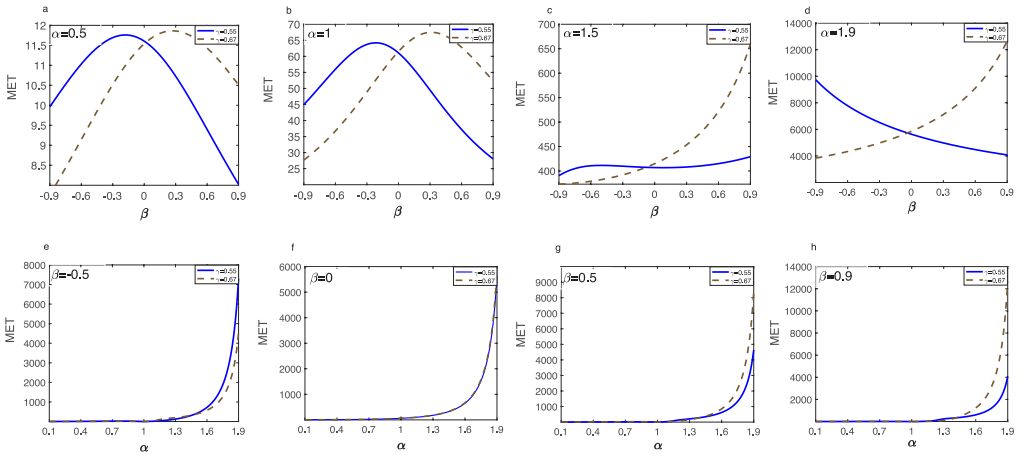


Figure 5. The dependence of α and β on MET is analysed for two stable cold states: $T_c = 240$ K for a strong greenhouse effect $\gamma = 0.55$ and $T_c = 228$ K for a weak one $\gamma = 0.67$, respectively. The skewness parameter β is varied within the range $[-0.9, 0.9]$ for the following fixed values of α: (a) $\alpha = 0.5$, (b) $\alpha = 1$, (c) $\alpha = 1.5$ and (d) $\alpha = 1.9$. Similarly, the stability parameter α is varied within the range $[0.1, 1.9]$ for the following fixed values of β: (e) $\beta = -0.5$, (f) $\beta = 0$, (g) $\beta = 0.5$ and (h) $\beta = 0.9$. In all cases, the noise intensity is fixed at $\epsilon = 0.5$.

noise ($\beta \neq 0$), a negative skewness noise reduces the stability of the climate system under a weak greenhouse effect. By contrast, when the noise skewness is positive, the stability of the system is enhanced, leading to the opposite conclusion.

From the perspective of climate change models, these findings reveal the nonlinear response mechanisms of the climate system to random perturbations. A stronger greenhouse effect intensifies the sensitivity of the climate system. It may also significantly decrease the stability of the cold state under specific noise conditions. This, in turn, increases the likelihood of transitions from the cold state to other climate states. This mechanism may manifest in real-world climate changes as an increased frequency of extreme climate events or irreversible shifts in the climate system. Therefore, studying the interaction between noise characteristics and greenhouse effects is crucial for understanding the long-term stability of the climate system and predicting future climate changes.

4. Conclusion

Abrupt climate change is a critical phenomenon in Earth's system dynamics, characterized by the rapid transitions between stable states. To investigate the underlying mechanisms, we employed a stochastic energy balance model that incorporates the influence of extreme weather events. In this framework, the MET serves as a deterministic measure to quantify the stability of climate states under stochastic fluctuations. A non-symmetric α-stable Lévy process was introduced to represent the effect of extreme, infrequent and large-scale climatic fluctuations.

The stability parameter α is a key measure capturing the frequency and intensity of extreme events. Our findings reveal that as α decreases, the MET decays significantly, indicating that the system requires less time to shift from the cold state to the warm one. Furthermore, as α approaches 2, the MET increases rapidly. This behaviour highlights the destabilizing influence of heavy-tailed noise with larger but less frequent jumps, which accelerates abrupt transitions and reduces the stability of the cold state.

The skewness parameter β determines the skewness of the α-stable Lévy random variable's distribution: it is left-skewed (with its tail extending to the left) when $\beta < 0$, and right-skewed (with its tail extending to the right) when $\beta > 0$. We conduct numerical analysis to examine MET

Downloaded from royalsocietypublishing.org/rsta/article-pdf/doi/10.1098/rsta.2024.0488/6160760/rsta.2024.0488.pdf
by guest
on 11 November 2026

trends with respect to β depending on α. This reveals that the variable of MET with respect to β presents a relatively consistent trend for systems characterized by larger jumps with low frequency ($\alpha < 1$) and those approaching the Gaussian noise limit, the trend for the intermediate value of α exhibits a strong dependence on β.

We further examined the variation trends of the MET for the cold state under two different intensities of greenhouse effects by introducing different noise characteristics. The results show that when the noise is symmetric, the stability of the climate system is similar regardless of the intensity of the greenhouse effect. However, when the noise is asymmetric, the stability is significantly affected: an enhanced greenhouse effect makes the cold state more sensitive to certain noise characteristics, thereby reducing its stability.

Data accessibility. This article has no additional data.

Declaration of AI use. We have not used AI-assisted technologies in creating this article.

Authors' contributions. Y.Z.: methodology, writing—original draft; H.X.: software, writing—review and editing; X.W.: validation, writing—review and editing; F.Y.: formal analysis, writing—review and editing; N.B.: conceptualization, writing—review and editing.

All authors gave final approval for publication and agreed to be held accountable for the work performed therein.

Conflict of interest declaration. We declare we have no competing interests.

Funding. N.B. acknowledges funding by the Volkswagen foundation. This is ClimTip contribution #X; the ClimTip project has received funding from the European Union's Horizon Europe research and innovation programme under grant agreement no. 101137601. F.Y acknowledges the National Natural Science Foundation of China (grant no. 12201639).

References

1. Ganopolski A, Rahmstorf S. 2001 Rapid changes of glacial climate simulated in a coupled climate model. *Nature* **409**, 153–158. (doi:10.1038/35051500)
2. Stommel H. 1961 Thermohaline convection with two stable regimes of flow. *Tellus* **13**, 224–230. (doi:10.1111/j.2153-3490.1961.tb00079.x)
3. Boers N, Ghil M, Stocker TF. 2022 Theoretical and paleoclimatic evidence for abrupt transitions in the Earth system. *Environ. Res. Lett.* **17**, 093006. (doi:10.1088/1748-9326/ac8944)
4. Wenjian H, Yiyang L, Huaping S, Taghizadeh-Hesary F. 2020 How does climate change affect rice yield in China?. *Agriculture* **10**, 441. (doi:10.3390/agriculture10100441)
5. Nazir MJ, Li G, Nazir MM, Zulfikar F, Siddique KHM, Iqbal B, Du Daolin. 2024 Harnessing soil carbon sequestration to address climate change challenges in agriculture. *Soil Tillage Res.* **237**, 105959. (doi:10.1016/j.still.2023.105959)
6. Dansgaard W, Clausen HB, Gundestrup N, Hammer CU, Johnsen SF, Kristinsdottir PM, Reeh N. 1982 A new greenland deep ice core. *Science* **218**, 1273–1277. (doi:10.1126/science.218.4579.1273)
7. North Greenland Ice Core Project members. 2004 High-resolution record of Northern Hemisphere climate extending into the last interglacial period. *Nature* **431**, 147–151. (doi:10.1038/nature02805)
8. Boers N, Ghil M, Rousseau DD. 2018 Ocean circulation, ice shelf, and sea ice interactions explain Dansgaard–Oeschger cycles. *Proc. Natl. Acad. Sci. USA* **115**, E11005–E11014. (doi:10.1073/pnas.1802573115)
9. Kindler P, Guillevic M, Baumgartner M, Schwander J, Landais A, Leuenberger M. 2014 Temperature reconstruction from 10 to 120 kyr b2k from the NGRIP ice core. *Clim. Past* **10**, 887–902. (doi:10.5194/cp-10-887-2014)
10. Ashwin P, Wieczorek S, Vitolo R, Cox P. 2012 Tipping points in open systems: bifurcation, noise-induced and rate-dependent examples in the climate system. *Philos. T. Roy. Soc. A* **370**, 1166–1184. (doi:10.1098/rsta.2011.0306)
11. Lenton TM, Held H, Kriegler E, Hall JW, Lucht W, Rahmstorf S, Schellnhuber HJ. 2008 Tipping elements in the Earth's climate system. *Proc. Natl. Acad. Sci. USA* **105**, 1786–1793. (doi:10.1073/pnas.0705414105)

Downloaded from royalsocietypublishing.org/rsta/article-pdf/doi/10.1098/rsta.2024.0488/6160760/rsta.2024.0488.pdf
by guest
on 11 November 2026

12. Chekroun MD, Simonnet E, Ghil M. 2011 Stochastic climate dynamics: random attractors and time-dependent invariant measures. *Phys. D Nonlinear Phenom.* **240**, 1685–1700. (doi:10.1016/j.physd.2011.06.005)
13. Bódai T, Tél T. 2012 Annual variability in a conceptual climate model: snapshot attractors, hysteresis in extreme events, and climate sensitivity. *Chaos Interdiscip. J. Nonlinear Sci.* **22**, 023110. (doi:10.1063/1.3697984)
14. National Research Council and Division on Earth and Life Studies and Board on Atmospheric Sciences and Committee on Understanding and Monitoring Abrupt Climate Change and Its Impacts. 2013 *Abrupt impacts of climate change: Anticipating surprises*. National Academies Press.
15. Hasselmann K. 1976 Stochastic climate models: part I. theory. *Tellus* **28**, 473–485. (doi:10.1111/j.2153-3490.1976.tb00696.x)
16. Cheong J, Sun J, Xu Min, Xin Z. 2023 Nondestructive detection of lipid oxidation in frozen pork using hyperspectral imaging technology. *J. Food Compos. Anal.* **123**, 105497. (doi:10.1016/j.jfca.2023.105497)
17. Zhu J, Jiang X, Rong Y, Wei W, Wu S, Jiao T, Chen Q. 2023 Label-free detection of trace level zearalenone in corn oil by surface-enhanced Raman spectroscopy (SERS) coupled with deep learning models. *Food Chem.* **414**, 135705. (doi:10.1016/j.foodchem.2023.135705)
18. Xu S *et al.* 2023 Monitoring leaf nitrogen content in rice based on information fusion of multi-sensor imagery from UAV. *Precis. Agric.* **24**, 2327–2349. (doi:10.1007/s11119-023-10042-8)
19. Ditlevsen PD. 1999 Observation of α-stable noise induced millennial climate changes from an ice-core record. *Geophys. Res. Lett.* **26**, 1441–1444. (doi:10.1029/1999gl900252)
20. Zheng Y, Yang F, Duan J, Sun X, Fu L, Kurths J. 2020 The maximum likelihood climate change for global warming under the influence of greenhouse effect and Lévy noise. *Chaos Interdiscip. J. Nonlinear Sci.* **30**, 013132. (doi:10.1063/1.5129003)
21. Applebaum D. 2009 *Lévy processes and stochastic calculus*. Cambridge, UK: Cambridge University Press. (doi:10.1017/cbo9780511809781)
22. Gardiner CW. 1985 *Handbook of stochastic methods*. Berlin, Germany: Springer.
23. Duan J. 2015 *An introduction to stochastic dynamics*. New York, NY: Cambridge University Press. (doi:10.1111/biom.12854)
24. Dshalalow J. 2005 On exit times of multivariate random walk with some applications to finance. *Nonlinear Anal. Theor. Methods Appl.* **63**, e569-e577. (doi:10.1016/j.na.2005.01.083)
25. Zheng Y, Serdukova L, Duan J, Kurths J. 2016 Transitions in a genetic transcriptional regulatory system under Lévy motion. *Sci. Rep.* **6**, 29274. (doi:10.1038/srep29274)
26. Lahti L, Salojärvi J, Salonen A, Scheffer M, de Vos Willem M. 2014 Tipping elements in the human intestinal ecosystem. *Nat. commun.* **5**, 4344. (doi:10.1038/ncomms5344)
27. Zheng Y, Boers N. 2023 Mean exit times as global measure of resilience of tropical forest systems under climatic disturbances—analytical and numerical results. *Chaos Interdiscip. J. Nonlinear Sci.* **33**, 113136. (doi:10.1063/5.0158109)
28. Gilbarg D, Trudinger NS. 1977 *Elliptic partial differential equations of second order*. New York, NY: Springer.
29. Oksendal B. 2013 *Stochastic differential equations: an introduction with applications*. Berlin, Germany: Springer.
30. Imkeller P, Pavlyukevich I, Wetzel T. 2009 First exit times for Lévy-driven diffusions with exponentially light jumps. *Ann. Probab.* **37**, 530–564. (doi:10.1214/08-aop412)
31. Imkeller P, Pavlyukevich I. 2006 Lévy flights: transitions and meta-stability. *J. Phys. A Math. Gen.* **39**, L237. (doi:10.1088/0305-4470/39/15/l01)
32. Gao T, Duan J, Li X, Song R. 2014 Mean exit time and escape probability for dynamical systems driven by Lévy noises. *SIAM J. Sci. Comput.* **36**, A887–A906. (doi:10.1137/120897262)
33. Wang X, Duan J, Li X, Song R. 2018 Numerical algorithms for mean exit time and escape probability of stochastic systems with asymmetric Lévy motion. *Appl. Math. Comput.* **337**, 618–634. (doi:10.1016/j.amc.2018.05.038)
34. Sato K. 1999 *Lévy processes and infinitely divisible distributions*. New York, NY: Cambridge University Press.
35. Yan H, Acquah SJ, Zhang J, Wang G, Zhang C, Darko RO. 2021 Overview of modelling techniques for greenhouse microclimate environment and evapotranspiration. *Int. J. Agric. Biol. Eng.* **14**, 1–8. (doi:10.25165/j.ijabe.20211406.3948)

Downloaded from royalsocietypublishing.org/rsta/article-pdf/doi/10.1098/rsta.2024.0488/6160760/rsta.2024.0488.pdf
by guest
on 11 November 2026

36. Kaper HG, Engler H. 2013 *Mathematics and climate*. Philadelphia, PA: Society for Industrial and Applied Mathematics (SIAM).
37. Saltzman B. 2002 *Dynamical paleoclimatology: generalized theory of global climate change* **80**. Academic Press.
38. Hansen J *et al.* 2005 Earth's energy imbalance: confirmation and implications. *Science* **308**, 1431–1435. (doi:/10.1126/science.1110252)
39. Ghil M, Lucarini V. 2020 The physics of climate variability and climate change. *Rev. Mod. Phys.* **92**, 035002. (doi:10.1103/revmodphys.92.035002)
40. Shaw TA *et al.* 2016 Storm track processes and the opposing influences of climate change. *Nat. Geosci.* **9**, 656–664. (doi:10.1038/ngeo2783)
41. Dijkstra HA. 2007 Characterization of the multiple equilibria regime in a global ocean model. *Tellus A Dyn. Meteorol. Oceanogr.* **59**, 695–705. (doi:10.1111/j.1600-0870.2007.00267.x)

Downloaded from royalsocietypublishing.org/rsta/article-pdf/doi/10.1098/rsta.2024.0488/6160760/rsta.2024.0488.pdf
by guest
on 11 November 2026